Use of Cavity Perturbation Techniques to Characterize Via-Plate Behavior

Tim Reeves, Michael Tsuk, Vishwanath Iyer
MathWorks, Inc. USA

***Abstract*— This paper describes an analytical technique for characterization of a via-plate assembly using a short-circuited coaxial resonant structure. Calculated via-plate coaxial and barrel plate capacitance values are compared to results previously published.**

***Keywords*— Coaxial resonator, Via-plate capacitance, mode matching technique, multi-layer structures.**

I. Introduction

Serial link communication systems are using increasingly higher data rates (28 and 56 Gbps). These communication systems make use of multilayer boards and signal traces are connected through different layers via metallized vertical vias [1] – [3]. The propagation of electrical signals through these multilayer interconnects excites parallel plate waveguide modes between plates separating dielectric layers. These excited modes can cause both undesirable signal integrity and power integrity effects that limit the use of multilayer circuit board assemblies. This warrants a simple, but effective full-wave electromagnetic analysis of these structures to understand the type of electromagnetic field propagation in these structures as well as any type of electromagnetic resonance supported by these assemblies.

A variety of full-wave electromagnetic as well as equivalent circuit analysis techniques have been used to characterize the behavior of via-plate assemblies. Electromagnetic analysis techniques such as FEM [4], FDTD [5], MoM [6] and mode matching analysis [7] have been used to characterize the via-plate behavior. Other analysis techniques make use of π-type lumped circuit model with excess inductance and capacitance [8]. Another method, the Foldy-Lax scattering technique combines electromagnetic modeling results with network theory methods to model multiple vias on multi-layer PCBs [2, 9]. The quasi-static integral equation method is also widely used to determine via-plate capacitance behavior. Physics-based via models have been used to determine via-plate capacitances, wherein a perfect magnetic conductor (PMC) boundary at the midpoint between the upper and lower parallel plates [10]. This analysis leads to determination of three separate capacitances, via-plate coaxial capacitance, via barrel-plate capacitance and fringing capacitances for the top and bottom of via segments.

In this paper, a simple, but rigorous mode matching analysis method is used to analyze not only the via-plate interaction but also extends the analysis to include the impact of enclosures on the behavior of the via-plate assembly. In addition, the formulation of the model supports analysis of equivalent perfect electric conductor (PEC) and perfect magnetic conductor (PMC) conditions at the axial midpoint of the parallel plate waveguide structures. This analysis will be useful for gaining insight into the electric and magnetic field behavior of the via-plate assemblies. As a resonance analysis of an enclosed structure is used, the need for excitation sources is unnecessary and the natural solution of the formulated model can be used to visualize the electromagnetic field solution and calculate equivalent circuit parameters such as capacitance and inductance. Calculated via-plate capacitances are compared against values tabulated from previous studies to demonstrate the accuracy of the formulation used herein.

II. Re-Entrant Coaxial Cavity for Via-Plate Analysis

Re-entrant coaxial cavities have been commonly used for dielectric material characterization as well as microwave heating applications. Since both coaxial cavities and printed circuit boards with thru vias each support TEM-like modes, it is proposed that a coaxial re-entrant structure would be useful for analysis of multilayer boards with signal vias. The TEM mode within the coaxial region would excite parallel plate waveguide modes of interest for via-plate characterization. Also, resonance analysis of these parallel plate waveguide structures is useful as data rates of serial communication systems are approaching the resonant frequencies of these parallel plate structures. In addition, the use of a resonant cavity analysis will also characterize the impact of upper and lower enclosure boundaries on the behavior of the via-plate structure. Analytical techniques mentioned in the previous section don't account for these enclosure effects.

To study different types of parallel-plate waveguide electromagnetic behavior, a short-circuited coaxial line, with a parallel plate waveguide placed at its axial center is selected. As a result of the symmetry of the enclosed structure, different virtual conditions (PMC and PEC) can be identified and analyzed via the mode matching technique.

With a virtual PMC at the axial center of the structure, odd-mode resonances result which occur at odd-integer multiples of half wavelengths supported by the short-circuited coaxial line. This type of resonance does not support any propagation within the parallel plate waveguide structure and field coefficients are for only odd-evanescent modes for this structural resonance condition.

With a virtual PEC at the axial center of the structure, even-mode resonances result which occur at even-integer multiples of half wavelengths supported by the short-circuited coaxial line. This type of resonance supports TEM

propagation within the parallel plate waveguide structure and field coefficients are dominated by the lowest order TEM mode.

III. Resonant Analysis Formulation

A. Anti-Pad to Air Region

In Figure 1, a cross-section of a cylindrical coaxial structure with a cylindrical parallel plate waveguide (filled with a dielectric material) placed at its axial center is depicted. The cylindrical parallel plate waveguide has a portion of its upper and lower metallization removed to create an anti-pad. As stated in the previous section, TEM-like modes are supported by this structure [11].

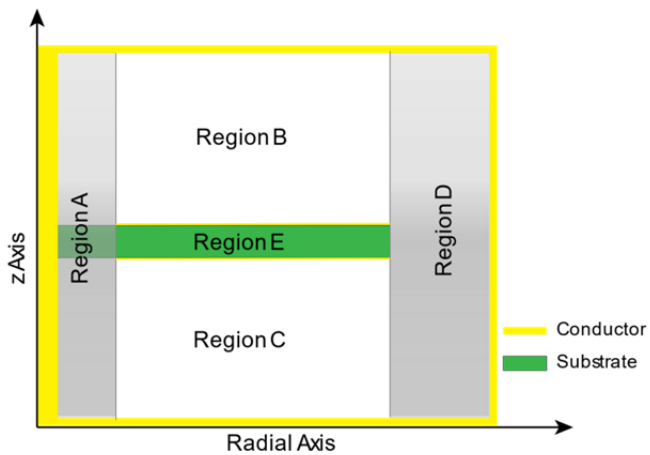

Figure 1. Cylindrical cross-section (r-z plane) of an enclosed coaxial cavity with a cylindrical single layer PCB with anti-pad at its axial center.

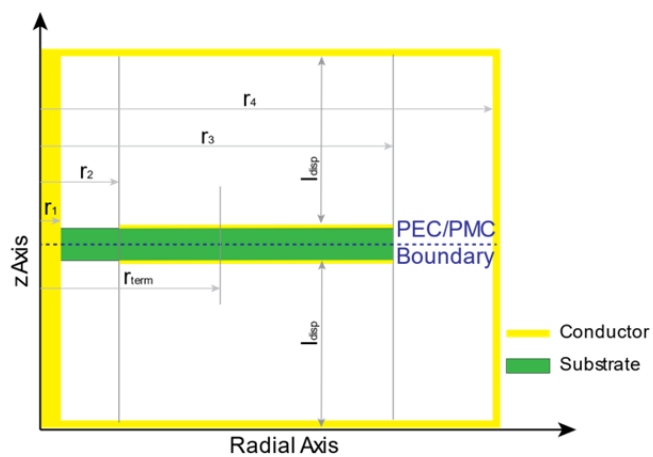

Figure 2. Depiction of subregions for the cylindrical cross-section of an enclosed coaxial cavity with a cylindrical single layer PCB with anti-pad at its axial center.

The Anti-Pad to Air region shown in Figure 1, can be treated as a multi-layer dielectric and axial mode matching can be used to determine the wave numbers in each subregion via eigenmode analysis [12].

As a result of the simplified analysis technique used, the following electric and magnetic fields can be represented in each region and take the general form:

$$E_z^i(r,z) = \sum_{n=0}^{N} a_n R_0^i(k_n^i r)\cosh\left(\beta_z^i(z+z_i)\right) \quad (1)$$

$$H_\phi^i(r,z) = \sum_{n=0}^{N} a_n \left(\frac{j\omega\varepsilon}{k_n^i}\right) R_1^i(k_n^i r)\cosh\left(\beta_z^i(z+z_i)\right) \quad (2)$$

$$E_r^i(r,z) = \sum_{n=1}^{N} a_n \left(\frac{\beta_z^i}{k_n^i}\right) R_1^i(k_n^i r)\sinh\left(\beta_z^i(z+z_i)\right) \quad (3)$$

where a_n are the field coefficients, R_0^i and R_1^i are radial functions dependent on the boundary conditions of each subregion, k_n^i are the radial wave numbers in each subregion, β_z^i are the axial wave numbers in each subregion and z_i are subregion start points relative to a base origin for the overall coaxial structure.

B. Subregion Radial Functions

To determine both the resonant frequency and field coefficients of each respective region, radial mode matching will be used at radial locations where discontinuities exist resulting from the geometrical structure being analyzed. In Figure 2, discontinuities in the axial direction occur at $r = r_2$ and $r = r_3$. In the subregions bounded by $r = r_1$, $r = r_2$, $r = r_3$ and $r = r_4$, different radial functions are used to describe the radial variation of each of the electric and magnetic fields within each of the subregions. A listing of the radial functions used in subregion is provided below.

<u>Regions A & D:</u>

$$R_0^i(k_n^i r) \in J_0^i(k_n^i r),\ Y_0^i(k_n^i r), I_0^i(k_n^i r), K_0^i(k_n^i r) \quad (4)$$
$$R_1^i(k_n^i r) \in J_1^i(k_n^i r),\ Y_1^i(k_n^i r), I_1^i(k_n^i r), K_1^i(k_n^i r) \quad (5)$$

<u>Regions B & C:</u>

$$R_0^i(k_n^i r) \in H_0^{(1)}(k_n^i r),\ H_0^{(2)}(k_n^i r), K_0^i(k_n^i r), K_0^i(-k_n^i r) \quad (6)$$
$$R_1^i(k_n^i r) \in H_1^{(1)}(k_n^i r), H_1^{(2)}(k_n^i r), K_1^i(k_n^i r), K_1^i(-k_n^i r) \quad (7)$$

<u>Region E:</u>

(no PEC termination between r_2 and r_3)

$$R_0^i(k_n^i r) \in H_0^{(1)}(k_n^i r),\ H_0^{(2)}(k_n^i r), K_0^i(k_n^i r), K_0^i(-k_n^i r) \quad (8)$$
$$R_1^i(k_n^i r) \in H_1^{(1)}(k_n^i r),\ H_1^{(2)}(k_n^i r), K_1^i(k_n^i r), K_1^i(-k_n^i r) \quad (9)$$

(PEC at radial position $r_2 < r_{term} < r_3$)

$$R_0^i(k_n^i r) \in J_0^i(k_n^i r),\ Y_0^i(k_n^i r), I_0^i(k_n^i r), K_0^i(k_n^i r) \quad (10)$$
$$R_1^i(k_n^i r) \in J_1^i(k_n^i r),\ Y_1^i(k_n^i r), I_1^i(k_n^i r), K_1^i(k_n^i r) \quad (11)$$

where J_m^i and Y_m^i are mth order Bessel functions of the first and second kind, I_m^i and K_m^i are mth order modified Bessel functions of the first and second kind and $H_m^{(1)}$ and $H_m^{(2)}$ are mth order Hankel functions of the first and second kind. Modified Bessel and Hankel functions are used when the radial wavenumber, k_n^i, is imaginary.

C. Field Coefficient Determination

To determine expressions for the field coefficients in each subregion, a Fourier Series expansion along the z-direction is required to obtain appropriate representations of Equations (1-3) in each respective subregion [11]. When the electric and magnetic field expressions are evaluated, with proper inner products being calculated, a square matrix of full rank is produced that can be used to determine resonant frequencies for the enclosed structure. As a result of the size of the matrix

required for accurate equivalent circuit element calculations, Singular Value Decomposition (SVD) rather than calculation of the matrix determinant is used to determine resonant frequency. With SVD, the number of field coefficients is not limited to a small number of values in each subregion. This leads to a more accurate representation of the electric and magnetic fields in each respective subregion.

IV. Numerical Results

A. Even-mode resonance

As pointed out in Section II, different resonant conditions occur with different virtual boundary conditions at the axial midpoint of the coaxial structure, and this results in different field configurations within the resonant structure. When an even-mode resonance occurs, TEM propagation occurs within the cylindrical parallel plate waveguide region and the lowest order mode for each of E_z and H_ϕ are dominant in Region E. In each of the A and D subregions, even order coefficients dominate the field expansion expressions for each of the electric and magnetic fields in each of these respective subregions.

B. Odd-mode resonance

When a virtual PMC occurs at the axial midpoint of the coaxial structure, an odd-mode resonance occurs. This type of resonance does not support wave propagation within the cylindrical parallel plate waveguide and evanescent field coefficients of odd order dominate in Region E. Also, in each of the A and D subregions, odd order coefficients dominate the field expansion expressions for the electric and magnetic fields.

C. Cylindrical plate waveguide resonance

One other type of resonance is supported within this structure as well, namely, the resonant condition of the cylindrical parallel plate waveguide region. When a PEC boundary is introduced between r_2 and r_3 a resonant mode will occur in the region between r_1 and r_{term}. The magnitude of the magnetic fields in the cylindrical parallel plate waveguide region is comparable to the magnitude of the magnetic fields within the coaxial region of the structure. Also, the axial electric fields in the cylindrical parallel plate waveguide structure are the dominant electric fields within the composite coaxial structure.

D. Validation of modeling technique

One way the modeling technique can be validated is through calculation of capacitance between the via and plate, namely, barrel, and coaxial capacitance. Via capacitance can be determined from odd-mode resonances. Once the resonant frequency is determined using SVD, the values of the Nth Right singular vector (where N is the mode matching formulation matrix order) are the coefficients for the electric and magnetic fields described in Equations (1 – 3). The barrel and coaxial capacitance can then be analytically determined using Gauss' law. The potential difference between the via and the plate can be analytically determined from integration of the radial electric field between the via and anti-pad. The electric flux can also be analytically determined from the radial electric field expansion via integration in the ϕ-z plane with the radial position fixed at either the via radius or the anti-pad radius points. Since the radial electric field can be expressed as an analytical function, and the field coefficients have been previously determined, the capacitance calculations can be computed quickly.

Results calculated using the resonant technique described in this paper can be compared against previously tabulated results [6]. In Table 1, a comparison of the barrel and coaxial capacitance computed via a Green's function analytical technique and the mode matching technique used herein are tabulated for a variety of via and anti-pad radii. For the results listed in the accompanying table, a total of 1000 modes are used in the stacked dielectric region, region A, as depicted in Figure 1 and the analysis is performed at a resonant frequency of approximately, $f_0 \sim 1.48$ GHz.

Another way that the results can be validated is to vary the via radius and compare that to previously reported results. In Figure 3, the anti-pad radius is set to 0.8mm, the plate separation is set to 0.254 mm (10 mil) and the plate thickness is set to 0.0254 mm (1 mil). Comparing the results plotted in this figure to Figure (14) as shown in [5] depicts a favorable comparison between the two techniques.

Making use of a resonant cavity technique permits for analysis of the impact that the upper and lower PEC boundaries have on the barrel and coaxial capacitance values calculated. Earlier results reported, were for the case when these boundaries are located at a large physical distance from the via and parallel plate structures ($l_{disp} \sim 150$mm) and the ratio of the PEC-parallel plate separation to the parallel plate separation is very large (ratio > 1000). As this ratio decreases, the coaxial capacitance increases, and the barrel capacitance decreases. In Figures 4 and 4a, this behavior is shown as a function of frequency for similar via and parallel plate separations as described in Figure 3.

V. Conclusion

A resonant cavity technique has been described for analysis of a via-plate assembly commonly used in high speed wired communications systems. It was found that three different types of quasi-TEM modes are supported in this structure and how these different resonances can be used to determine equivalent capacitance and inductance parameters. The analytical technique described was used to determine equivalent capacitance for the via-plate assembly and the results favorably compared to previously reported results. Since an enclosed assembly was analyzed, the impact of upper and lower PEC boundaries near the via-plate assembly could also be determined.

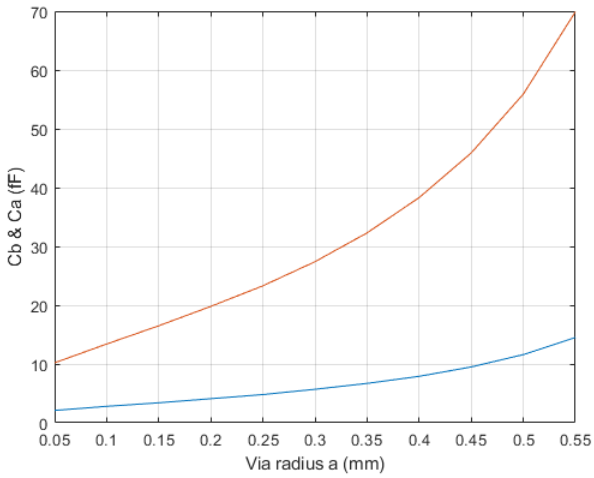

Fig.3. Barrel-plate and coaxial capacitances versus the via radius with fixed antipad radius and via height (b = 0.8 mm, h = 0.254 mm, t = 0.0254 mm, ε_r = 3.84)

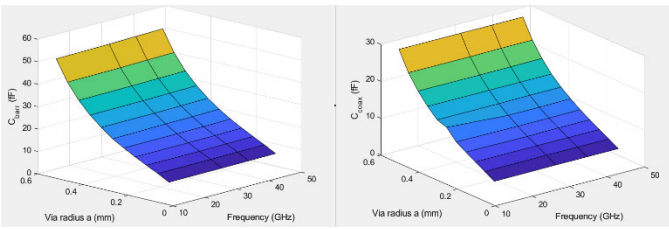

Fig. *4a and 4b*. Barrel-plate and coaxial capacitance as a function of frequency and via radius for a PEC boundary to plate separation of 17.4 mm. Dimensions are like those given in Figure 3.

Table 1. Comparison of the Via-Plate Capacitance Value Calculated using Mode-Matching and those tabulated in reference (1). ($h_u = h_d$ = 0.2286mm (9 mil), t = 0.0254 mm (1 mil), ε_r = 3.84)

case	**radii (mm)**		**C_{via} (fF)**	
	a	b	Ref (1)	Mode Matching technique
1	0.1016	0.3556	42.6	42.7
2	0.1016	0.4318	37.2	37.3
3	0.1016	0.5080	33.4	33.9
4	0.1524	0.3556	61.7	62.7
5	0.1524	0.4318	51.2	51.6
6	0.1524	0.5080	44.6	44.9
7	0.2032	0.3556	89.6	93.2
8	0.2032	0.4318	69.9	70.5
9	0.2032	0.5080	58.4	60.0

REFERENCES

[1] E. Laermans, J. Geest, D. Zutter, F. Olyslager, S. Sercu, and D. Morlion, "Modeling complex via hole structure," *IEEE Trans. Adv. Packag.*, vol. 25, no. 2, pp. 206–214, May 2002.

[2] H. Chen, Q. Lin, L. Tsang, C.-C. Huang, and V. Jandhyala, "Analysis of a large number of vias and differential signaling in multilayered structures," *IEEE Trans. Microw. Theory Tech.*, vol. 51, no. 3, pp. 818–829, Mar. 2003.

[3] Y. Zhang, J. Fan, G. Selli, and M. Cocchini, "Analytical Evaluation of Via-Plate Capacitance for Multilayer Printed Circuit Boards and Packages," *IEEE Trans. Microw. Theory Tech.*, vol. 56, pp. 2118-2128, September 2008.

[4] P. Kok and D. Zutter, "Capacitance of a circular symmetric model of a via hole including finite ground plane thickness," *IEEE Trans. Microw. Theory Tech.*, vol. 39, no. 7, pp. 1229–1234, Jul. 1991.

[5] T. Wang, R. F. Harington, and J. R. Mautz, "Quasi-static analysis of a microstrip via through a hole in a ground plane," *IEEE Trans. Microw. Theory Tech.*, vol. 36, no. 6, pp. 1008–1013, Jun. 1988.

[6] S.-G. Hsu and R.-B.Wu, "Full-wave characterization of a through hole via in multilayered packaging," *IEEE Trans. Microw. Theory Tech.*, vol. 43, no. 5, pp. 1073–1081, May 1995.

[7] H.H. Park, C. Hwang, K-Y. Jung and Y.B. Park, "Mode Matching Analysis of Via-Plate Capacitance in Multilayer Structures with Finite Plate Thickness," *IEEE Trans. on Elec. Comp.*, vol. 57, pp. 1188-1195, October 2015.

[8] T. Wang, R. F. Harington, and J. R. Mautz, "Quasi-static analysis of a microstrip via through a hole in a ground plane," *IEEE Trans. Microw. Theory Tech.*, vol. 36, no. 6, pp. 1008–1013, Jun. 1988.

[9] H. Chen, Q. Lin, L. Tsang, C.-C. Huang, and V. Jandhyala, "Analysis of a large number of vias and differential signaling in multilayered structures," *IEEE Trans. Microw. Theory Tech.,* vol. 51, no. 3, pp. 818–829, Mar. 2003.

[10] R. Rimolo-Donadio, X. Gu, Y. H. Kwark, M. B. Ritter, B. Archambeault, F. de Paulis, Y. Zhang, J. Fan, H.-D. Bruns, and C. Schuster, "Physics based via and trace models for efficient link simulation on multilayer structures up to 40 GHz," *IEEE Trans. Microw. Theory Tech*., vol. 57, no. 8, pp. 2072–2082, Aug. 2009.

[11] M. Steinberger, D. Telian, M. Tsuk, and V. Iyer, "Proper Ground Return Via Placement for 40+ Gbps Signaling," technical presentation, DesignCon 2022.

[12] T. Shen, K.A. Zaki, C. Wang, "Tunable Dielectric Resonators with Dielectric Tuning Disks," *IEEE Trans. Microw. Theory Tech.,* vol. 48, pp. 2439-2445, December 2000.